

# Application of Dispersion and Regression Analysis for Studying the Relationships of Some Components of Upper Pliocene Sediments of the Indian Ocean

K. V. Syromyatnikov<sup>a, \*</sup> and M. A. Levitan<sup>a</sup>

<sup>a</sup>*Vernadsky Institute of Geochemistry and Analytical Chemistry, Russian Academy of Sciences, Moscow, 119991 Russia*

*\*e-mail: sykirv@gmail.com*

Received October 30, 2019; revised March 3, 2020; accepted March 4, 2020

**Abstract**—The variance and regression analyses were applied to study the distribution and relationships between organic carbon, calcium carbonate, abiogenic matter, biogenic silica, and their accumulation depth in the upper Pliocene sediments in different structural zones of the Indian Ocean. Analysis of variance allowed us to quantify the influence of diverse facies settings on the distribution of sedimentation components. For the first time, linear and nonlinear regression models of the relationships between organic carbon, calcium carbonate, abiogenic matter, biogenic silica, and their accumulation depth are presented.

**Keywords:** bottom sediments, Indian Ocean, Upper Pliocene, organic carbon, calcium carbonate, abiogenic matter, analysis of variance, regression analysis

**DOI:** 10.1134/S0016702921020075

## INTRODUCTION

One of the widest spread methods of study of bottom sediments and suspended particulate matter of modern seas and oceans is the determination of their component composition, in particular, analysis of abiogenic (lithogenic) matter (AM),  $\text{CaCO}_3$ ,  $\text{SiO}_2$  biog., and  $\text{C}_{\text{org}}$ . Obtained results are expressed in weight percents or in absolute masses expressed in  $(\text{g}/\text{cm}^2)$  ka. The studies traditionally involve the determination of the components and their relationships, for instance, with primary production, bottom depth, and matter fluxes on the floor, and others (Lisitsyn et al., 1974, 1978; Levitan, 1992; van Andel et al., 1975; Farrell et al., 1995).

The study of relationship of sediment-forming components with each other and with main facies factors of sedimentation environment highlights an increasing need in their complex analysis. The development of numerical modeling provoked numerous publications on multiple correlation of results of component analysis (Costa et al., 2018).

In this work, the analysis of variance and regression analyses were applied to the component analysis of Upper Pliocene sediments from the DSDP cores in the Indian Ocean.

## FACTUAL ANALYSIS AND ANALYTICAL METHODS

This paper is based on data obtained during DSDP cruises nos. 22–27 in the Indian Ocean (von der

Borch et al., 1974; Whitmarsh et al., 1974; Fisher et al., 1974; Simpson et al., 1974; Davies et al., 1974; Veevers et al., 1974). The contents and mass accumulation rates of the above mentioned components in the Late Pliocene sediments (Table 1) were calculated in (Levitan et al., 2018a, 2018b, 2018c) using data on cores presented in the aforementioned reports on deep-water drilling. In this region (Fig. 1, Table 1), 18 landforms of the Indian ocean floor were studied based on 26 deep-water holes.

It is pertinent to mention that  $\text{CaCO}_3$  and  $\text{C}_{\text{org}}$  were determined using LECO analyzer during cruises and are expressed in weight percents. The indicated contents of  $\text{SiO}_2$  biog. in % were calculated by counting the areas occupied by siliceous organisms (mainly diatoms and radiolarian, with less common silicoflagellates and sponge spicules) in thin sections (smear slides). Special studies showed that starting from 30% the  $\text{SiO}_2$  biog. content determined under microscope is approximately 20% higher than the true content of this component determined with chemical analysis (Uliana et al., 2001). The content of abiogenic matter equals the difference between 100% and total  $\text{CaCO}_3$ ,  $\text{SiO}_2$  biog. and  $\text{C}_{\text{org}}$  in percents. Contents and mass accumulation rates of  $\text{SiO}_2$  biog. shown in Table 1 are reported for the first time.

Mass accumulation rates were calculated using data on stratigraphy, humidity, and density of natural sediments and the rate of their sedimentation presented in reports.

**Table 1.** The average contents (%) and mass accumulation rates (mar, g/cm<sup>2</sup> thou years) of calcium carbonate (CaCO<sub>3</sub>), biogenic silica (SiO<sub>2</sub> biog.), abiogenic matter (AM), and organic carbon (C<sub>org</sub>) in the Upper Pliocene sediments of different structures of the Indian Ocean

| Structures                            | Hole, No. | Hole coordinates latitude/longitude | Structure type* | C <sub>org</sub> , % | C <sub>org</sub> <sup>mar</sup> | CaCO <sub>3</sub> , % | CaCO <sub>3</sub> <sup>mar</sup> | AM, % | AM <sup>mar</sup> | SiO <sub>2</sub> biog., % | SiO <sub>2</sub> biog. <sup>mar</sup> (mar × 100) | Depth, m |
|---------------------------------------|-----------|-------------------------------------|-----------------|----------------------|---------------------------------|-----------------------|----------------------------------|-------|-------------------|---------------------------|---|----------|
| Wharton Basin                         | 211       | 09°46.53' S<br>102°41.95' E         | 1               | 0.2                  | 0.00174                         | 1                     | 0.009                            | 39    | 0.3391            | 60                        | 52.14   | 5528     |
| Ninety East Ridge                     | 217       | 08°55.57' N<br>90°32.33' E          | 2               | 0.2                  | 0.00211                         | 62                    | 0.66                             | 38    | 0.4013            | 0.01                      | 0.01  | 3030     |
| Chagos–Lakkadive Ridge                | 219       | 9°01.75' N<br>72°52.07' E           | 2               | 0.01                 | 0.0001                          | 63                    | 0.69                             | 37    | 0.4078            | 0.01                      | 0.011   | 1764     |
| Arabian Basin                         | 222       | 20°05.49' N<br>61°30.56' E          | 1               | 0.3                  | 0.0872                          | 14                    | 4.07                             | 86    | 25                | 0.01                      | 0.29  | 3546     |
| Continental slope of the Somali Ocean | 223       | 18°44.98' N<br>60°07.78' E          | 3               | 2.2                  | 0.0268                          | 21                    | 0.26                             | 72    | 0.8775            | 4.8                       | 5.85  | 3633     |
| Gulf of Aden                          | 232       | 14°28.93' S<br>51°54.87' E          | 3               | 0.6                  | 0.0376                          | 22                    | 1.38                             | 76    | 3.7571            | 2                         | 12.52   | 1743     |
| Gulf of Aden                          | 233       | 14°19.68' N<br>52°08.11' E          | 3               | 2.1                  | 0.2578                          | 43                    | 5.28                             | 49    | 6.0152            | 5.9                       | 72.43   | 1839     |
| Somali Basin                          | 235       | 03°14.06' N<br>52°41.64' E          | 1               | 0.5                  | 0.0286                          | 53                    | 3.03                             | 42    | 2.4033            | 5                         | 28.61   | 5130     |
| Central Indian Ridge                  | 238       | 11°09.21' S<br>70°31.56' E          | 2               | 0.1                  | 0.0001                          | 93                    | 3.59                             | 2     | 0.0773            | 5                         | 19.32   | 2832     |
| Mascarene Basin                       | 239       | 21°17.67' S<br>51°40.73' E          | 1               | 0.1                  | 0.000441                        | 12                    | 0.05                             | 88    | 0.3881            | 0.01                      | 0.004   | 4971     |
| Continental slope of Somali           | 241       | 02°22.24' S<br>44°40.77' E          | 3               | 0.3                  | 0.00918                         | 54                    | 1.65                             | 44    | 1.3464            | 2                         | 6.12  | 4054     |
| Davi Ridge                            | 242       | 15°50.65' S<br>41°49.23' E          | 2               | 0.2                  | 0.01389                         | 55                    | 3.82                             | 45    | 3.1248            | 0.01                      | 0.069   | 2275     |
| Mozambique Basin                      | 248       | 29°31.78' S<br>37°28.48' E          | 1               | 0.4                  | 0.021427                        | 19                    | 1.02                             | 81    | 4.339             | 0.01                      | 0.054   | 4994     |
| Mozambique Basin                      | 250       | 33°27.74' S<br>39°22.15' E          | 1               | 0.5                  | 0.01797                         | 5                     | 0.18                             | 94    | 3.3791            | 1                         | 3.594   | 5119     |

Table 1. (Contd.)

| Structures                   | Hole, No. | Hole coordinates latitude/longitude | Structure type* | C <sub>org</sub> , % | C <sub>org</sub> (mar) | CaCO <sub>3</sub> , % | CaCO <sub>3</sub> (mar) | AM, % | AM (mar) | SiO <sub>2</sub> biog., % | SiO <sub>2</sub> biog. (mar × 100) | Depth, m |
|------------------------------|-----------|-------------------------------------|-----------------|----------------------|------------------------|-----------------------|-------------------------|-------|----------|---------------------------|------------------------------------|----------|
| Africa-Antarctic Ridge       | 251       | 36°30.26' S<br>49°29.08' E          | 2               | 0.4                  | 0.02105                | 86                    | 4.52                    | 12    | 0.6314   | 2                         | 10.51                              | 3849     |
| Krozet Basin                 | 252       | 37°02.44' S<br>59°14.33' E          | 1               | 0.2                  | 0.00297                | 0.1                   | 0.001                   | 57    | 0.8464   | 42.9                      | 42.9                               | 5032     |
| Ninety East Ridge            | 253       | 24°52.65' S<br>87°21.97' E          | 2               | 0.01                 | 0.0001                 | 97                    | 0.44                    | 3     | 0.0127   | 0.01                      | 0.005                              | 1962     |
| Ninety East Ridge            | 254       | 30°58.15' S<br>87°53.72' E          | 2               | 0.1                  | 0.000182               | 96                    | 0.175                   | 4     | 0.0073   | 0.01                      | 0.002                              | 1253     |
| Naturaliste plateau          | 258       | 33°47.69' S<br>112°28.42' E         | 3               | 0.6                  | 0.01356                | 86                    | 1.9443                  | 9     | 0.2035   | 5                         | 11.3                               | 2793     |
| Timor deep-water trough      | 262       | 10°52.19' S<br>123°50.78' E         | 3               | 0.5                  | 0.0209                 | 72                    | 3.51                    | 27    | 1.1267   | 1                         | 4.88                               | 2298     |
| Wharton Basin                | 263       | 23°19.43' S<br>110°58.81' E         | 1               | 0.1                  | 0.003                  | 84                    | 2.93                    | 16    | 0.5572   | 0.01                      | 0.04                               | 5048     |
| Naturaliste Plateau          | 264       | 34°58.13' S<br>112°02.68' E         | 3               | 0.01                 | 0.0001                 | 100                   | 0.64                    | 0     | 0        | 0.01                      | 0.006                              | 2876     |
| Southeastern Mid-Ocean Ridge | 265       | 53°32.45' S<br>109°56.74' E         | 2               | 0.01                 | 0.0001                 | 7                     | 0.58                    | 1     | 0.009    | 90                        | 745.7                              | 3581     |
| Southeastern Mid-Ocean Ridge | 266       | 56°24.13' S<br>110°06.70' E         | 2               | 0.01                 | 0.0001                 | 1                     | 0.04                    | 9     | 0.09     | 90                        | 360                                | 4167     |
| Australian-Antarctic Basin   | 267       | 59°15.74' S<br>104°29.30' E         | 1               | 0.01                 | 0.0001                 | 0                     | 0                       | 80    | 0.63     | 20                        | 0                                  | 4522     |
| Continental foot             | 268       | 63°56.99' S<br>105°09.34' E         | 3               | 0.01                 | 0.0001                 | 0                     | 0                       | 97    | 1.15     | 3                         | 0                                  | 3529     |

\* Morphological structures of the Indian ocean floor are shown by numerals: (1) deep-water basins; (2) submarine ridges and rises; (3) continental margins.

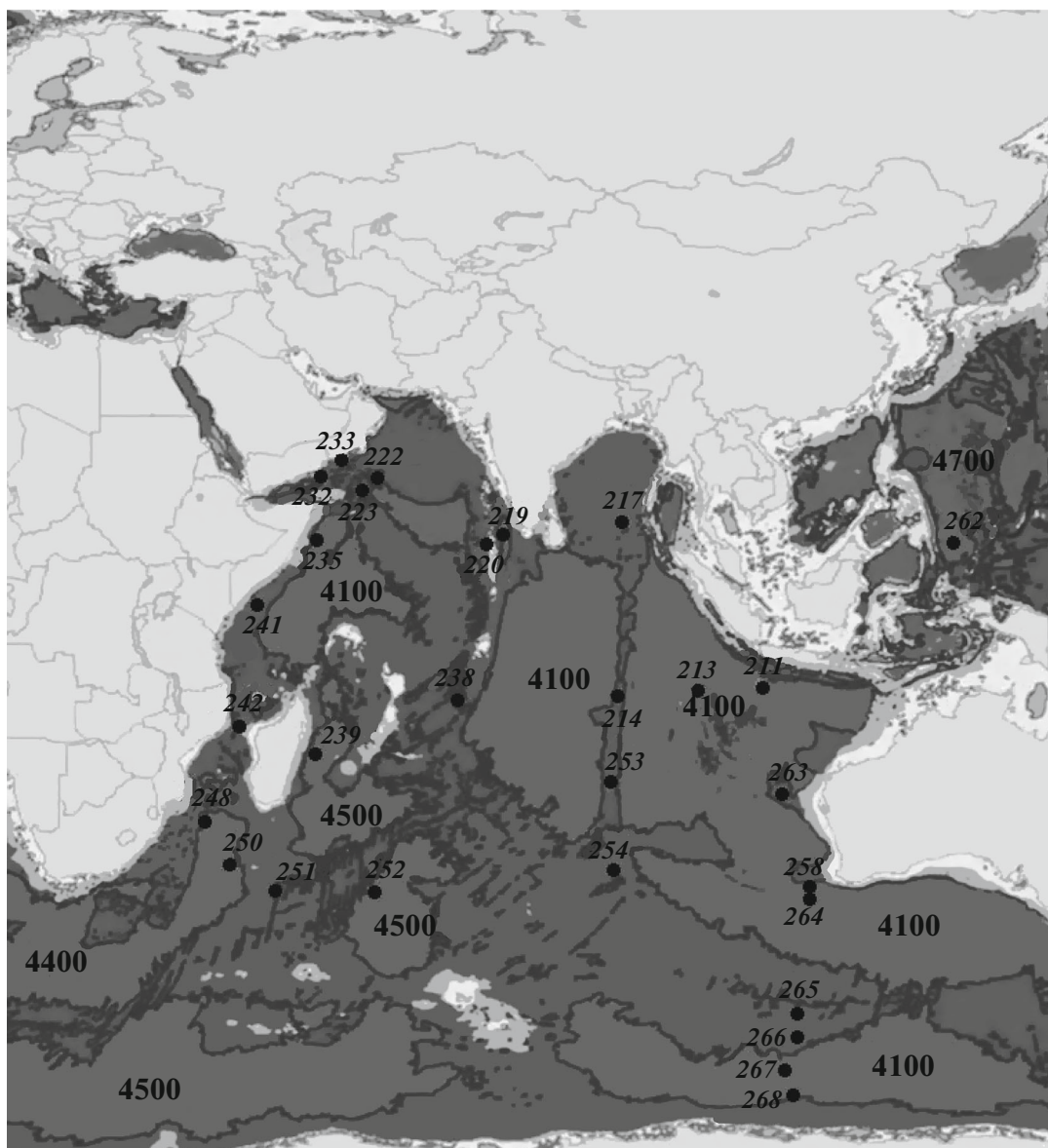


**Fig. 1.** Location of DSDP holes in the Indian Ocean shown on a fragmentary map of the deep-water basins of the World Ocean from paper (modified after Harris et al., 2014). Italic shows hole numbers, 4100–4700 are depths of deep-water basins (in m).

In spite of the plate tectonic motions, the probable changes of paleocoordinates and bottom depths of the studied holes were taken to be insignificant. Therefore, Table 1 lists the present-day coordinates and bottom depths.

The Upper Pliocene sediments experienced diagenetic alterations, which, however, were much weaker than in older sediments (Levitan, 1992). Therefore, we suggest that sedimentation signal in components reported in Table 1 is expressed much stronger than diagenetic signal.

There is one more important fact related to the qualitative parameters of the studied components. All components are heterogeneous. In particular,  $C_{org}$

contains organic carbon of both terrigenous and planktonogenic origin. A priori clear that the relative role of terrigenous organic matter is higher in the deposits of the Bengal and Indian fans (deep-water fans of the great Ganges and Brahmaputra rivers and Indus River).  $CaCO_3$  in sediments in the influence zone of the Zambezi River and so on is mainly represented by planktonic (foraminifers and coccolithophores) skeletons, whereas tropical zones contain pteropod remains at relatively shallow depths, and shelves are abundant in remains of mollusks and echinoderms; Oman shelf contains terrigenous detrital carbonates. The composition of  $SiO_2$  biog. was mentioned above. Abiogenic matter includes terrigenous sedimentary material, volcanogenic-detrital, terrigenous–volcanogenic, as well

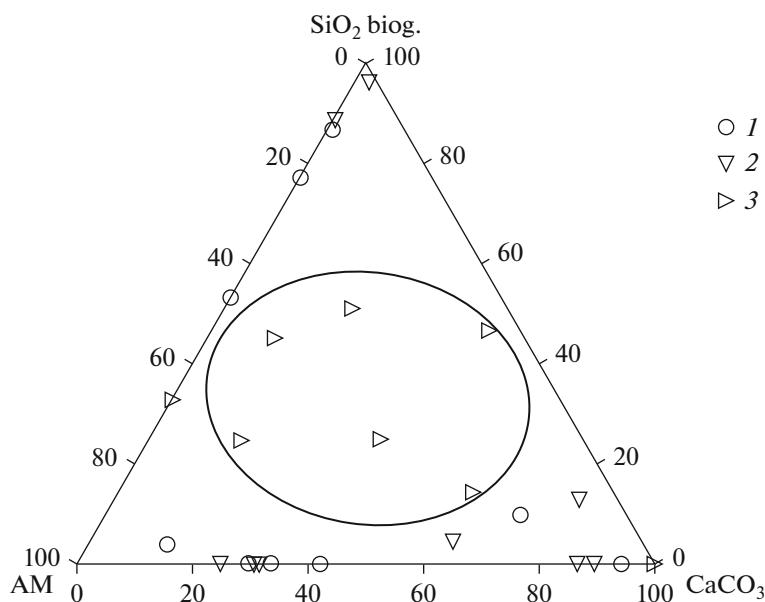


**Fig. 2.** Triangular diagram of  $\text{CaCO}_3$ ,  $\text{SiO}_2$  biog. and abiogenic matter (AM) in the Upper Pliocene sediments of the Indian Ocean (in percents). Symbols: (1) deep-water basins; (2) submarine ridges and rises; (3) continental margins.

as abiogenic matter of pelagic red clays. The abiogenic matter represents an insoluble carbonate residue with great fraction of authigenic minerals.

Statistical processing of data was carried out using a Statgraphics plus 5.0 software.

## RESULTS

**Triangle abiogenic matter,  $\text{CaCO}_3$ ,  $\text{SiO}_2$  biog.** All results presented in Table 1 (except for  $C_{\text{org}}$ ) are shown in percents in the abiogenic matter (AM)– $\text{CaCO}_3$ – $\text{SiO}_2$  biog. triangular diagram (Fig. 2). Analysis of the diagram indicates that only components of Late Pliocene sediments accumulated on the continental slopes of the Indian Ocean form a single cluster (contoured by a solid line). The components of sediments from abyssal floor, i.e., deep-water basins and diverse ridges and rises, are confined in composition to two-component mixtures of abiogenic matter and  $\text{CaCO}_3$ , on the one hand, and abiogenic matter and biogenic silica, on the other. This indicates that the components of abyssal sediments are sharply differentiated into siliceous–lithogenic and carbonate–lithogenic groups. It is possible that “two oceans” identified for Pleistocene (Levitan, 2016) also have existed in the Late Pliocene: “ice-bearing” (i.e., Indian Ocean part of the South Ocean, in the given case, siliceous–lithogenic group) and “ice-free” (ascribed to the low and moderate latitudes, carbonate–lithogenic group).

**Results of analysis of variance.** The analysis of variance is aimed at determining the significant influence of definite qualitative or quantitative factor on the

change of the studied resultative feature. For this purpose, factor supposedly having or not having significant influence is divided into gradation classes (or groups) and significance between the average values in data sets corresponding to the factor gradations is analyzed to determine the factor influence.

In this paper, we applied one-way analysis of variance, i.e., method testing the effect of a single independent variable on a dependent variable.

The distribution of biogenic and abiogenic matter was studied in more detail using a one-way analysis of variance data on the abiogenic matter, calcium carbonate, biogenic silica, and organic carbon (Fig. 3a). It was established that the distribution of abiogenic and biogenic matter depends on its facies affiliation: with confidence level of 95% for abiogenic matter (Fig. 3b), with confidence level of 99% for calcium carbonate (Fig. 3c), and with confidence level of 95% for organic carbon (Fig. 3d).

The distribution of abiogenic matter was controlled by the laws of mechanical differentiation, i.e., according to size of detrital particles, as well as was determined by the morphometric features of the considered structures of the Indian Ocean floor (Figs. 1, 3a, 3b). Our studies showed that the maximum concentrations of abiogenic matter in sediments are observed on the continental slope and in basins, which is related to the maximum sedimentation rates on the continental slopes overlain by terrigenous sediments and in the deep-water basin areas subjected to the influence of mud flows and submarine landslides from adjacent continental slopes. In addition, the high AM concentrations in the deep floor area accumulating red clays

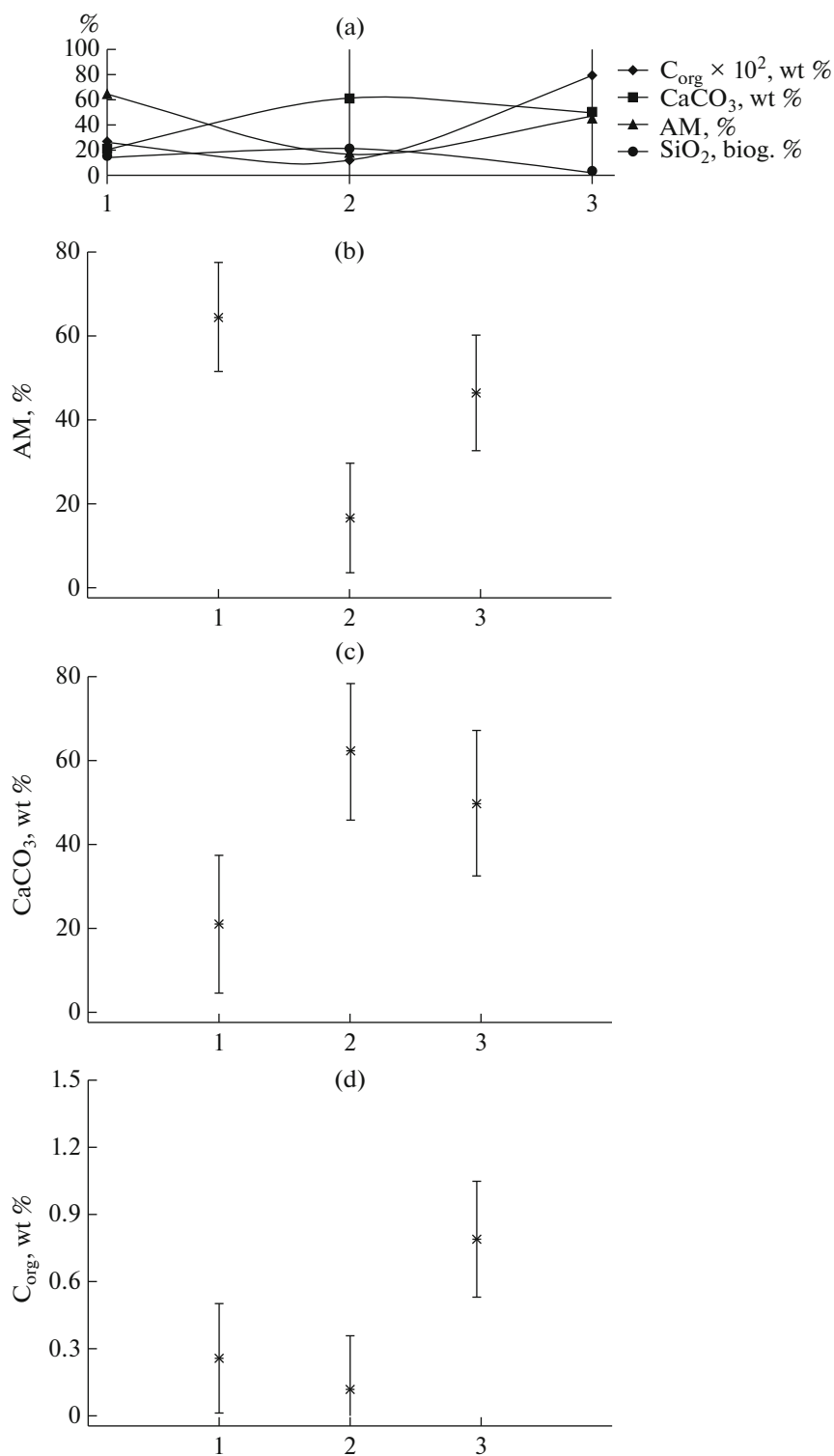


**Fig. 3.** Distribution of the average contents of major components of sediments (in percents) in main facies regions according to the analysis of variance: (a) summary profile; (b) average values and 95% confidence intervals of AM distribution; (c) average values and 99% confidence intervals of  $CaCO_3$  distribution; (d) average values and 95% confidence intervals of  $C_{org}$  distribution. (1) deep-water basins; (2) submarine ridges and rises; (3) continental margins.

**Table 2.** Summary data on polynomial regression relationship between  $C_{org}$  and AM

| Independent variables               | Coefficients of the regression equation | Precision error of regression equation | Student t-test       | <i>P</i> -value    |                 |
|-------------------------------------|---|--|----------------------|--------------------|-----------------|
| CONSTANT                            | −0.0102                                 | 1.0101                                 | −0.014               | 0.321              |                 |
| AM                                  | 0.026                                   | 0.00594                                | 4.31                 | 0.0003             |                 |
| AM                                  | −0.00086                                | 0.000239                               | −3.60419             | 0.0015             |                 |
| Dispersion                          | Sum of squares                          | Number of freedom degree               | Estimated dispersion | Fisher's criterion | <i>P</i> -value |
| Regression dispersion               | 0.0334667                               | 2                                      | 0.0167               | 11.55              | 0.0003          |
| Discrepancy                         | 0.0333153                               | 23                                     | 0.00145              |                    |                 |
| Total dispersion                    | 0.066782                                | 25                                     |                      |                    |                 |
| Determination coefficient           |   |  | 50.11%               |                    |                 |
| Corrected determination coefficient |   |  | 45.78%               |                    |                 |
| Standard error                      |   |  | 0.038                |                    |                 |
| Average absolute error              |   |  | 0.02                 |                    |                 |
| Durbin–Watson statistics            |   |  | 2.12                 |                    |                 |

are caused by the absence of carbonates due to their dissolution. The lowest contents of abiogenic matters are noted on rises where AM is diluted by carbonates.

Analysis of calcium carbonate distribution in sediments (Figs. 3a, 3c) showed that its high contents are restricted to submarine ridges and continental slopes, while the lowest contents, to basins. The maximum concentrations of carbonates on the submarine ridges and rises are mainly determined by a weak influence of diluting AM, as well as by the elevated production of  $CaCO_3$  and its minimum dissolution at shallow depths. Significant role is played by sediments predominating on continental margin. Therefore, the continental margins of the Arabian Peninsula and Australia (the latter are beyond the scope of our analysis) are occupied by carbonates of different composition and show high  $CaCO_3$  contents. Owing to the circum-continental zoning in the distribution of primary production, these areas show the highest carbonate productivity. In the abyssal basins below the carbonate compensation depth (CCD), carbonates are dissolved.

The distribution of  $C_{org}$  in the Upper Pliocene sediments (Figs. 3a, 3d) indicates its highest values on the continental margins owing to the mentioned circum-continental zoning of primary production. In addition, the abundant fine sedimentary material accumulating in this facies setting serves as sorbent for organic matter. At the same time, a mechanism of “biological pump” provides transportation of AM through planktonic organisms on the floor (Lisitsyn, 1978). The  $C_{org}$  concentrations in abyssal sediments are much lower than on the continental margins due to the decrease of primary production and a relative increase of sediment grain size on submarine ridges, which is related to the extraction of  $C_{org}$ -bearing fine sedimentary material by bottom currents.

**Results of the regression analysis.** The regression analysis is successfully applied in oceanology for studying the distribution of diverse components of sediments in different facies settings. For instance, it was applied to map the  $C_{org}$  content in sediments of different facies (Costa et al., 2018) or to analyze the distribution of organic carbon in the surface sediments in Ubatuba Bay (Burone et al., 2003).

The relationships between calcium carbonate, organic carbon abiogenic matter, biogenic silica, and their accumulation depths were analyzed using one-way regression analysis. The relationships were estimated for the following pairs: (1)  $C_{org}$  and abiogenic matter (AM) (in mass accumulation rates ( $g/cm^2$ ) ka); (2)  $C_{org}$  and  $CaCO_3$  (in percents) (3)  $CaCO_3$  (in percents) vs. accumulation depth; (4)  $CaCO_3$  and AM (in percents); (5)  $SiO_2$  biog. and  $CaCO_3$  (in percents).

The study of the first pair,  $C_{org}$  and AM (Table 2), by a polynomial regression allowed us to found a statistically significant relationship between two variables at 99% level, which is confirmed by *P*-value less than 0.01 (Table 2). In the given case, the determination coefficient ( $R^2$ ) is 50.11% and represents the proportion of the variance in the dependent variable  $C_{org}$  that is predictable from the independent variable AM, which is explained by the constructed regression model. Standard regression error (mean squared deviation of regression residual) is 0.038. This value represents a standard deviation of observed  $C_{org}$  from predictable  $C_{org}$ . The polynomial regression equation has the following form:

$$C_{org} = -0.0102 + 0.026AB - 0.00086AB^2.$$

The relationship between mass accumulation rates of  $C_{org}$  and AM (Fig. 4a) indicates that at relatively low (up to 5–7 ( $g/cm^2$ ) ka) mass accumulation rates of AM, the

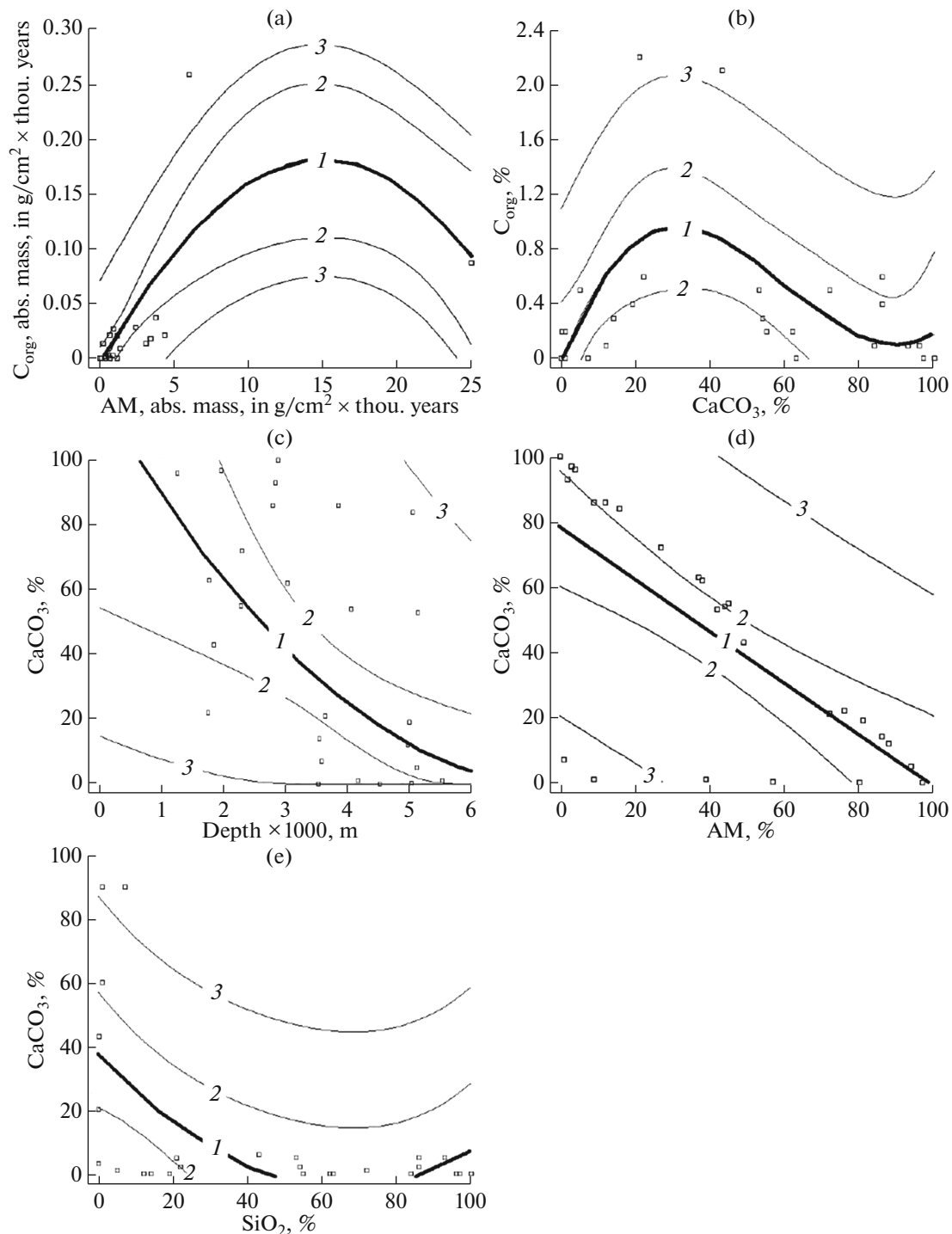


**Fig. 4.** Results of regression analysis: (a) plot of polynomial regression plot for relationships between mass accumulation rates of  $C_{org}$  and AM (in  $g/cm^2$  thou years); (b) plot of polynomial regression for relationship between  $C_{org}$  and  $CaCO_3$  (in wt %); (c) plot of non-linear inverse relationship between  $CaCO_3$  (in wt %) and hole depth (in m); (d) plot of non-linear inverse relationship between  $CaCO_3$  (in wt %) and AM (in %); (e) plot of non-linear opposite relationship between  $CaCO_3$  (in wt %) and  $SiO_2$  biog. (in %). (1) regression line; (2) confidence interval for the average values of predicted regression values; (3) confidence interval corresponding to the predicted regression value.

components show a positive correlation, which is likely caused by absorption of dissolved organics by essentially pelitic material of AM. At the same time, the right-hand part of the figure suggests that at ultrahigh mass accu-

mulation rates of AM ( $>15$  ( $g/cm^2$ ) ka), the predominant part of this material does not absorb dissolved OM, since it has been already precipitated on AM and therefore dilutes the lesser part of AM, which absorb  $C_{org}$ .



**Table 3.** Summary data on polynomial regression of  $C_{org}$  and  $CaCO_3$  regression

| Independent variables               | Beta coefficient | Precision error of regression equation | Student's t-test |                    | P-value |
|-------------------------------------|------------------|--|------------------|--------------------|---------|
| CONSTANT                            | 0.015            | 0.21                                   | -0.07            |                    | 0.94    |
| $CaCO_3$                            | 0.0702           | 0.027                                  | 2.65             |                    | 0.015   |
| $CaCO_3^2$                          | -0.002           | 0.0007                                 | -2.225           |                    | 0.035   |
| $CaCO_3^3$                          | -0.0000084       | 0.000005                               | 1.85             |                    | 0.08    |
| Dispersion                          | Sum of squares   | Number of freedom degree               | Dispersion       | Fisher's criterion | P-value |
| Regression dispersion               | 2.48             | 3                                      | 0.83             | 3.4                | 0.035   |
| Discrepancy                         | 5.35             | 22                                     | 0.24             |                    |         |
| Total dispersion                    | 7.82             | 25                                     |                  |                    |         |
| Determination coefficient           |                  |  | 32%              |                    |         |
| Corrected determination coefficient |                  |  | 22.3%            |                    |         |
| Standard error                      |                  |  | 0.5              |                    |         |
| Average absolute error              |                  |  | 0.3              |                    |         |
| Durbin-Watson statistics            |                  |  | 2.2              |                    |         |

The regression polynomial study revealed a statistically significant relationship between variables  $C_{org}$  and  $CaCO_3$  in wt % (Fig. 4b, Table 3) with a 95% confidence level, which confirms  $P$ -value < 0.05. The determination coefficient of 32% suggests that the dependent variable  $C_{org}$  has changed by this value under the influence of the independent variable  $CaCO_3$ . The standard error is 0.5 (Table 3). The polynomial regression best fits the equation:

$$C_{org} = -0.015 + 0.0702CaCO_3 - 0.0015CaCO_3^2 + 0.0000084CaCO_3^3.$$

The relationship between  $C_{org}$  and  $CaCO_3$  in the Upper Pliocene sediments (Fig. 4b) shows a complex dependence. It shows a tight positive correlation at low values (up to 30%  $CaCO_3$ ), which can be interpreted by simultaneous accumulation of both components on continental margins (Fig. 3a). At calcium carbonate contents from 30 to 80%, correlation is negative, which likely indicates a dilution of organic matter in a setting of submarine ridges and rises. A trend of positive correlation at high (>80%  $CaCO_3$ ) contents could be explained by the presence of specific organic matter in calcitic shells at extremely low contents of other organic varieties (partially, owing to the removal of this organics with fine sediment fractions in the crest zones of the ridges and rises, Table 1). According to last data, the  $C_{org}$  contents in sediments of submarine ridge could be lowered also owing to its intense consumption by bacteria inhabiting mud waters (Sunita et al., 2018). At the same time, the same relations are also observed in other facies conditions: on the conti-

ental margins of the Arabian Peninsula (Table 1). They are controlled by different mechanisms: accumulation of carbonate deposits in the absence of terrigenous flux (except for aeolian material) and the elevated  $C_{org}$  in sediments owing to upwelling (Levitan, 1992).

The  $CaCO_3$  (%) shows a moderately negative correlation with accumulation depth (m) (Fig. 4c), at correlation coefficient of -0.6 (Table 4). The  $P$ -value < 0.01 and equal 0.004 (Table 4) confirms a relationship between  $CaCO_3$  and depth at a statistic significance of 99%. The determination coefficient in this regression model is 30.3%. Thereby, a standard error is 2.97. The calcium carbonate in sediments shows a significant decrease at depths from 4500 to 5000 meters (Fig. 4c). The correlation of  $CaCO_3$  versus depth is determined by non-linear equation:

$$CaCO_3 = (10.9406 - 0.0015D)^2,$$

where  $D$  is the depth  $\times$  1000, m.

Obtained data should be interpreted as a result of  $CaCO_3$  dissolution with depth, and the mentioned change in its content within 4500–5000 m is clearly related to the known acceleration of carbonate dissolution with approaching the carbonate compensation depth (Lisitsyn, 1978).

The study of regression for  $CaCO_3$  and AM (values are given in relative percents) indicates their mutual dilution, which is proved with a significance level of 99% (Fig. 4d, Table 5). Thereby,  $P$ -value is less than 0.01 (Table 5). The determination coefficient of 50.3% shows a proportion of variance of the dependent variable  $CaCO_3$  under the influence of the independent variable AM. Thereby, the standard regression error is 2.91. The dependence of  $CaCO_3$  variable versus abio-

**Table 4.** Summary data on regression analysis of CaCO<sub>3</sub> and depth relations. Equation of non-linear regression:  $Y = (a + bX)^2$ 

| Parameters                          | Coefficients of the polynomial regression equation | Standard errors in estimated coefficients | Student's <i>t</i> -test |                    | <i>P</i> -value |
|-------------------------------------|--|---|--------------------------|--------------------|-----------------|
| <i>a</i>                            | 10.9406  | 1.73                                      | 6.32                     |                    | 0.00            |
| <i>b</i>                            | -0.0015  | 0.0005                                    | -3.23                    |                    | 0.004           |
| Dispersion                          | Sum of squares                                     | Number of freedom degree                  | Dispersion               | Fisher's criterion | <i>P</i> -value |
| Regression dispersion               | 92.08  | 1   | 92.08                    | 10.4               | 0.004           |
| Discrepancy                         | 212.27   | 24  | 8.84                     |                    |                 |
| Total dispersion                    | 304.35   | 25  |                          |                    |                 |
| Correlation coefficient             |  |   |                          | -0.6               |                 |
| Determination coefficient           |  |   |                          | 30.3               |                 |
| Corrected determination coefficient |  |   |                          | 27.4%              |                 |
| Standard error                      |  |   |                          | 2.97               |                 |
| Average absolute error              |  |   |                          | 2.39               |                 |
| Durbin-Watson statistics            |  |   |                          | 1.26               |                 |

**Table 5.** Summary data on regression analysis of relationships between CaCO<sub>3</sub> and abiogenic matter (AM). Equation of linear regression:  $Y = a + bX$ 

| Parameters                          | Regression coefficient | Standard errors in estimated coefficients | Student's <i>t</i> -test |                    | <i>P</i> -value |
|-------------------------------------|------------------------|---|--------------------------|--------------------|-----------------|
| <i>a</i>                            | 77.8702                | 8.6                                       | 9.05                     |                    | 0.000           |
| <i>b</i>                            | -0.793                 | 0.16                                      | -4.93                    |                    | 0.000           |
| Dispersion                          | Sum of squares         | Number of freedom degree                  | Dispersion               | Fisher's criterion | <i>P</i> -value |
| Regression dispersion               | 17048.6                | 1   | 17048.6                  | 24.28              | 0.000           |
| Discrepancy                         | 16850.4                | 24  | 702.1                    |                    |                 |
| Total dispersion                    | 33899                  | 25  |                          |                    |                 |
| Correlation coefficient             |                        |   |                          | -0.71              |                 |
| Determination coefficient           |                        |   |                          | 50.3               |                 |
| Corrected determination coefficient |                        |   |                          | 48.2%              |                 |
| Standard error                      |                        |   |                          | 26.5               |                 |
| Average absolute error              |                        |   |                          | 17.98              |                 |
| Durbin-Watson statistics            |                        |   |                          | 1.28               |                 |

genic matter (AM) can be described by the linear regression equation:

$$\text{CaCO}_3 = 77.8702 - 0.793\text{AM}.$$

The polynomial regression study of the relations between biogenic silica (%) and CaCO<sub>3</sub> (%) revealed their statistical relationships at a significance level of 99%, which is confirmed by *P*-value of 0.007 (Table 6). The relations between two variables is shown in Fig. 4e. The determination coefficient is 35.3% (Table 6), which explains the proportion of variance in the dependent variable SiO<sub>2</sub> biog. owing to variance of the

independent variable CaCO<sub>3</sub>. The relationships of SiO<sub>2</sub> biog. dependence with CaCO<sub>3</sub> can be described by the polynomial regression equation:

$$\text{SiO}_2 \text{ biog.} = 37.6361 - 1.261\text{CaCO}_3 + 0.0096\text{CaCO}_3^2.$$

Analysis of Fig. 4e shows that these variables have a negative correlation at SiO<sub>2</sub> biog. from 0 to 60–70% and a positive correlation at higher SiO<sub>2</sub> biog. Thus, the components dilute each other in the first case (in most facies settings), while accelerated dissolution of

**Table 6.** Summary data on polynomial regression of SiO<sub>2</sub> biog. (%) and CaCO<sub>3</sub> (wt %) relationships

| Independent variables               | Beta coefficient |                          | Precision error of regression equation | Student's <i>t</i> -test | <i>P</i> -value |
|-------------------------------------|------------------|--------------------------|--|--------------------------|-----------------|
| CONSTANT                            | 37.6361          |                          | 8.26                                   | 4.56                     | 0.0001          |
| CaCO <sub>3</sub>                   | -1.261           |                          | 0.49                                   | -2.59                    | 0.016           |
| CaCO <sub>3</sub> <sup>2</sup>      | 0.0096           |                          | 0.005                                  | 1.91                     | 0.07            |
| Dispersion                          | Sum of squares   | Number of freedom degree | Dispersion                             | Fisher's criterion       | <i>P</i> -value |
| Regression dispersion               | 6263.7           | 3                        | 3131.9                                 | 6.3                      | 0.007           |
| Discrepancy                         | 11494.2          | 22                       | 499.75                                 |                          |                 |
| Total dispersion                    | 17757.9          | 25                       |  |                          |                 |
| Determination coefficient           |                  |                          |  | 35.3%                    |                 |
| Corrected determination coefficient |                  |                          |  | 29.6%                    |                 |
| Standard error                      |                  |                          |  | 22.4                     |                 |
| Average absolute error              |                  |                          |  | 14.3                     |                 |
| Durbin–Watson statistics            |                  |                          |  | 1.3                      |                 |

carbonates in the second case (at maximum depths of abyssal basins in the South Ocean) eliminates their diluting role for biogenic SiO<sub>2</sub>.

## CONCLUSIONS

Mutual correlation methods were used to analyze the contents of major components (C<sub>org</sub>, CaCO<sub>3</sub>, abiogenic matter, and SiO<sub>2</sub> biog.) in the Upper Pliocene sediments of the Indian Ocean recovered in 26 DSDP holes.

It is established that major components (AM, CaCO<sub>3</sub>, and SiO<sub>2</sub> biog.) can be divided into three groups based on their relationships: (1) three-component association confined to continental margins and forming a compact cluster; (2) two-component mixture of abiogenic matter and CaCO<sub>3</sub>, and (3) two-component mixture of abiogenic matter and biogenic silica. The second and third groups are restricted to the abyssal floor: the second group is restricted to the moderate and low latitudes, while the third group, to the Indian Ocean sector of the South Ocean.

Obtained data agree well with classical concepts on the distribution of abiogenic and biogenic material in oceanic settings. Thereby, one-way analysis of variance revealed that the distribution of abiogenic and biogenic materials clearly depends on their facies affiliation.

The application of one-way regression analysis (with presentation of linear and non-linear regression equations, which consider the relationships of components with 95–99% statistical significance) allowed us to estimate reliably the component analysis data and to unravel previously unknown features, for instance, in the distribution of C<sub>org</sub> depending on the mass accumulation rates of AM and percentage of

CaCO<sub>3</sub>, as well as relations between the percentages of CaCO<sub>3</sub> and SiO<sub>2</sub> biog.

Obtained tendencies can be used in developing the numerical models of the Late Pliocene sedimentation in the Indian Ocean.

## FUNDING

This paper was supported by the Russian Foundation for Basic Research (project no. 08-05-00221).

## REFERENCES

- L. Burone, P. Muniz, A. M. S. Pires-Vanin, and M. Rodrigues, "Spatial distribution of organic matter in the surface sediments of Ubatuba Bay," *J. An. Acad. Bras. Sci.* **75** (1), 75–90 (2003).
- E. M. Costa, W. S. Tassinari, H. S. K. Pinheiro, S. J. Beutler, and L. H. C. Dos Anjos Mapping soil organic carbon and organic matter fractions by geographically weighted regression, *J. Environ. Qual.* **47** (4), 718–725 (2018).
- T. A. Davies, B. P. Luyendyk, et al., *DSDP Init. Repts.* **26**, (1974)
- J. W. Farrell, I. Raffi, T. R. Janecek, D. W. Murray, M. A. Levitan, K. A. Dadley, K.-C. Emeis, M. Lyle, J.-A. Flores, and S. Hovan, "Late Neogene sedimentation patterns in the eastern equatorial Pacific," In: *Proc. ODP, Sci. Results* **138**, 717–756 (1995).
- R. L. Fisher, E. T. Bunce, et al., *DSDP Init. Repts.* **24**, (1974).
- P. T. Harris, M. Macmillan-Lawler, J. Rupp, and E. K. Baker, "Geomorphology of the oceans," *Mar. Geol.* **352**, 4–24 (2014).
- M. A. Levitan, *Paleoceanology of the Indian Ocean* (Nauka, Moscow, 1992) [in Russian].

- M. A. Levitan, "Comparative analysis of pelagic pleistocene silica accumulation in the Pacific and Indian oceans," *Geochem. Int.* **54** (3), 257–265 (2016).
- M. A. Levitan, L. G. Domoratskaya, and A. V. Koltsova, "History of organic carbon accumulation," *Quantitative Parameters of the Mesozoic–Cenozoic Sedimentation: Essays*, Ed. by M. A. Levitan (Pero, Moscow, 2018a), pp. 15–40 [in Russian].
- M. A. Levitan, L. G. Domoratskaya, and A. V. Koltsova, "History of carbonate accumulation," *Quantitative Parameters of the Mesozoic–Cenozoic Sedimentation: Essays*, Ed. by M. A. Levitan (Pero, Moscow, 2018b), pp. 62–97 [in Russian].
- M. A. Levitan, L. G. Domoratskaya, and A. V. Koltsova, "History of terrigenous sedimentation," *Quantitative Parameters of the Mesozoic–Cenozoic Sedimentation: Essays*, Ed. by M. A. Levitan (Pero, Moscow, 2018c), pp. 98–124 [in Russian].
- A. P. Lisitsyn, *Sedimentation in Oceans. Quantitative Distribution of Sedimentary Material* (Nauka, Moscow, 1974) [in Russian].
- A. P. Lisitsyn, *Oceanic Sedimentation. Lithology and Geochemistry* (Nauka, Moscow, 1978) [in Russian]
- E. S. Simpson, W. R. Schlich, et al., DSDP Init. Repts. **25**, (1974).
- R. Sunita, S. Walter, U. Jaekel, H. Osterholz, A. T. Fisher, J. A. Huber, A. Pearson, Th. Dittmar, and P. R. Girguis, "Microbial decomposition of marine dissolved organic matter in cool oceanic crust," *Nature Geosci.* **11**, 334–339 (2018).
- E. Uliana, C. B. Lange, B. Donner, and G. Wefer, "Siliceous phytoplankton productivity fluctuations in the Congo Basin over the past 460000 years: marine vs. riverine influence, ODP Site 1077," *Proc. ODP, Sci. Results* **175**, 1–32 (2001).
- T. H. van Andel, C. R. Heath, and T. C. Moore, "Cenozoic tectonics, sedimentation and paleoceanography of the central equatorial Pacific," *Geol. Soc. Amer. Mem.* **143**, 1–65 (1975).
- J. J. Veevers, J. R. Heirtzler, et al., DSDP Init. Repts. **27**, (1974).
- Ch. C. von der Borch, J. G. Sclater, et al., DSDP Init. Repts. **22**, (1974).
- R. B. Whitmarsh, O. E. Weser, D. A. Ross, et al., DSDP Init. Repts. **23**, (1974).

*Translated by M. Bogina*